



Effect of X on the transport properties of skutterudites $\text{LaFe}_4\text{X}_{12}$ (X = P, As and Sb) compounds



A.H. Reshak ^{a, b, *}

^a New Technologies – Research Centre, University of West Bohemia, Univerzitni 8, 306 14 Pilsen, Czech Republic

^b Center of Excellence Geopolymer and Green Technology, School of Material Engineering, University Malaysia Perlis, 01007 Kangar, Perlis, Malaysia

ARTICLE INFO

Article history:

Received 9 July 2015

Received in revised form

13 August 2015

Accepted 14 August 2015

Available online 17 August 2015

Keywords:

Filled skutterudite

Transport properties

Electronic band structure

Boltztrap code

ABSTRACT

We have investigated the influence of substituting P by As and As by Sb on the thermoelectric properties of $\text{LaFe}_4\text{X}_{12}$ (X = P, As and Sb) compounds. It has been found that substituting $\text{P} \rightarrow \text{As} \rightarrow \text{Sb}$ show significant influence on the bands dispersions, bond lengths, effective masses, the carriers mobility and hence the transport properties. Replacing P by As cause significant increases in the carriers concentration with increasing the temperatures, while replacing As by Sb exhibit insignificant increase in the carriers concentration of $\text{LaFe}_4\text{Sb}_{12}$ with respect to $\text{LaFe}_4\text{As}_{12}$. It is clear that $\text{LaFe}_4\text{As}_{12}$ show the highest electrical conductivity among the other compounds along the temperature range. Calculations show that $\text{LaFe}_4\text{Sb}_{12}$ exhibit low electronic thermal conductivity in the temperature range between 50 and 600 K, then above 650 K the $\text{LaFe}_4\text{P}_{12}$ compound show the lower electronic thermal conductivity. The Seebeck coefficient of $\text{LaFe}_4\text{X}_{12}$ (X = P, As and Sb) compounds increases with increasing the temperature. Moving from $\text{P} \rightarrow \text{As} \rightarrow \text{Sb}$ cause significant increases in the Seebeck coefficient and $\text{LaFe}_4\text{Sb}_{12}$ compound exhibit the highest Seebeck coefficient along whole temperature scale. The power factor of $\text{LaFe}_4\text{X}_{12}$ (X = P, As and Sb) compounds increases with increasing the temperature and $\text{LaFe}_4\text{Sb}_{12}$ compound show the highest power factor along the whole temperature range.

© 2015 Elsevier B.V. All rights reserved.

1. Introduction

The filled skutterudite compounds are promising candidates for thermoelectric applications [1] due to their high carrier mobility, low lattice thermal conductivity and low electrical resistivity [1–3]. Several interesting phenomena have been observed in these materials, for instance semiconductivity [4,5], superconductivity [6–8], magnetic order [9–13], metal-insulator transition material [14] and valence fluctuation and heavy fermion behavior [15–17]. Among the filled skutterudite compounds are the La-based filled skutterudite phosphide, arsenide and antimonide [18,19]. These materials possess extremely large figure of merit ($ZT = S^2\sigma T/k$) [20,21]. The thermoelectric figure of merit is used to determine the efficiency of the materials which used for thermoelectric application. Where S is Seebeck coefficient, σ the electrical conductivity and $k = k_e + k_l$ is the thermal conductivity which consists of two

parts, the electronic and phonon (lattice) parts. To gain efficient thermoelectric materials therefore, we have to reduce the thermal conductivity. Much efforts were taken to reduce the lattice thermal conductivity part during filling of the empty icosahedral cages site in the skutterudite structure with rare earth atoms [22,23]. Nouneh et al. [24] have investigated the temperature dependence of the resistivity, Seebeck coefficient and photoinduced second harmonic generation near the quantum critical point in the skutterudite compound $\text{LaFe}_4\text{Sb}_{12}$.

To date, there exist a number of band structure calculations for $\text{LaFe}_4\text{X}_{12}$ (X = P, As and Sb) compounds using different methods within the local density approximation (LDA) and generalized gradient approximation (GGA) as exchange and correlation potentials. The band structure and Fermi surface of $\text{LaFe}_4\text{X}_{12}$ (X = P, As and Sb) compounds were calculated within density functional theory (DFT) [25]. The full potential linear augmented plane wave (FP-LAPW) method within the local density approximation (LDA) was used to investigate the band structure of simple cubic $\text{LaRu}_4\text{P}_{12}$ and the orthorhombic $\text{LaFe}_4\text{P}_{12}$ compounds, the Fermi surface and the hybridization between La-f orbital and P-p states were investigated [26]. Hachemaoui et al. [27] report an *ab initio* calculation

* New Technologies – Research Centre, University of West Bohemia, Univerzitni 8, 306 14 Pilsen, Czech Republic.

E-mail address: maalidph@yahoo.co.uk.

using LDA to investigate the structural and elastic properties of $\text{LaFe}_4\text{X}_{12}$ ($\text{X} = \text{P, As and Sb}$) compounds. A complex band structure calculations for $\text{LaFe}_4\text{Sb}_{12}$ and $\text{CeFe}_4\text{Sb}_{12}$ compounds was performed using tight-binding linear muffin-tin orbital (TB-LMTO) and full potential linear augmented plane wave (FPLAPW) methods to calculate the density of states near Fermi level and the corresponding thermoelectric properties [22]. It is well known that for the highly correlated compounds, LDA and GGA are fail to give the correct ground state. In these systems, the electrons are highly localized. The Coulomb repulsion between the electrons in open shells should be taken into account [28]. To the best of our knowledge there is dearth information on the transport properties of $\text{LaFe}_4\text{X}_{12}$ ($\text{X} = \text{P, As and Sb}$) compounds. Therefore, this motivates us to address ourselves for a comprehensive theoretical calculation using the all-electron full potential linear augmented plane wave plus the local orbitals (FPLAPW+*lo*) method within the recently modified Becke–Johnson potential (mBJ) [29] to calculate the transport properties of $\text{LaFe}_4\text{X}_{12}$ ($\text{X} = \text{P, As and Sb}$) compounds based on the band structure calculations. The modified Becke–Johnson potential allows the calculation with accuracy similar to the very expensive GW calculations [29]. It is a local approximation to an atomic “exact-exchange” potential and a screening term. In the recent years due to the improvement of the computational technologies, it has been proven that the first-principles calculation is a strong and useful tool to predict the crystal structure and its properties related to the electron configuration of a material before its synthesis [30–34].

2. Details of calculations

This work is devoted to study the influence of substituting P by As and As by Sb on the thermoelectric properties of skutterudites $\text{LaFe}_4\text{X}_{12}$ ($\text{X} = \text{P, As and Sb}$) compounds. To achieve this it is essential to have reliable electronic energy band structure parameters determining the carriers mobility and the carriers occupation in the vicinity of Fermi level (E_F). The reliable transport properties can be obtained from accurately calculated electronic structure. Therefore, electronic transport coefficients of skutterudites $\text{LaFe}_4\text{X}_{12}$ ($\text{X} = \text{P, As and Sb}$) compounds are evaluated by means of the semi-classical Boltzmann theory and rigid band model. Based on the electronic band structure calculations the thermoelectric properties of the $\text{LaFe}_4\text{X}_{12}$ ($\text{X} = \text{P, As and Sb}$) compounds are obtained utilizing the semi-classical Boltzmann theory as implemented in the BoltzTraP code [32]. In BoltzTraP code the relaxation time (τ) taken to be direction independent and isotropic [35,36].

$\text{LaFe}_4\text{X}_{12}$ ($\text{X} = \text{P, As and Sb}$) compounds crystallizes in cubic space group $Im\bar{3}$. In the unit cell, La atom is situated at (0.0, 0.0, 0.0), Fe at (0.25, 0.25, 0.25) and X at (0.0, *u*, *v*) [18,19]. In our previous work [37] the ground state properties of $\text{LaFe}_4\text{X}_{12}$ ($\text{X} = \text{P, As and Sb}$) compounds were calculated using the all-electron full potential linear augmented plane wave (FPLAPW + *lo*) method as implemented in Ref. WIEN2k code [38]. The lattice constant *a* and the two internal free parameters *u* and *v* were optimized by minimizing the total energy [37]. The optimization is achieved using the local density approximation (LDA) [39]. From the relaxed geometry of $\text{LaFe}_4\text{X}_{12}$ ($\text{X} = \text{P, As and Sb}$) compounds we have calculated the ground state properties and hence the thermoelectric properties using the recently modified Becke–Johnson potential (mBJ) [29], which optimizes the corresponding potential for electronic band structure calculations. To solve the Kohn–Sham equations a basis of linear APW's are used. In the muffin-tin (MT) spheres the potential and charge density are expanded in spherical harmonics with $l_{\text{max}} = 8$ and nonspherical components up to $l_{\text{max}} = 6$. In the interstitial region the potential and the charge density are represented by Fourier series. In order to achieve energy

eigenvalues convergence, the wave functions in the interstitial region are expanded in terms of plane waves with a cut-off of $K_{\text{MAX}} = 8/R_{\text{MT}}$. Self-consistency is obtained using 800 *k* points in the irreducible Brillouin zone (IBZ). The self-consistent calculations are converged since the total energy of the system is stable within 10^{-5} Ry. The transport coefficients are calculated using 15,000 *k* points in the IBZ.

3. Results and discussion

3.1. Salient features of the electronic band structures and density of states

It is clear that from Fig. 1 the bands just below Fermi level (E_F), shifts towards Fermi level when we substitute $\text{P} \rightarrow \text{As} \rightarrow \text{Sb}$. This cause significant influence on the bands locations below and above E_F resulting in some modification in the ground state properties and increase the density of states at Fermi level ($N(E_F)$). These bands consist of Fe-3d and X-p bands which show weak hybridization. Substitute $\text{P} \rightarrow \text{As} \rightarrow \text{Sb}$ also cause increasing/reducing the parabolic shape of the bands in the vicinity of E_F resulting in lower/increase the effective mass and hence increase/reduce the mobility of the carriers. Substituting $\text{P} \rightarrow \text{As} \rightarrow \text{Sb}$ lead to increase the bond lengths and angles resulting in the reducing of orbital splitting [37]. As a result, the bonding states shift towards the higher energy level. Meanwhile, the energy level of the anti-bonding states will be enhanced. It is interesting to mention that due to the small electronegativity differences between P, As and Sb therefore, substituting $\text{P} \rightarrow \text{As} \rightarrow \text{Sb}$ will not introduce more peaks in the density of states and no extra charge will be attracted towards As or Sb when we replace P by As and As by Sb [40]. To show this influence we have illustrated the electronic band structure of $\text{LaFe}_4\text{X}_{12}$ ($\text{X} = \text{P, As and Sb}$) compounds in the energy region between 0.2 and -0.2 eV (the region where these compounds expected to give maximum efficiency), together with the carriers concentration as a function of $(\mu - E_F)$ between -0.2 and $+0.2$ eV at three constant temperatures (300, 600 and 900) K as shown in Fig. 1(a)–(c). The difference between chemical potential and Fermi energy ($\mu - E_F$) is positive for valence bands and negative for conduction bands. It is clear from the electronic band structure that $\text{LaFe}_4\text{X}_{12}$ ($\text{X} = \text{P, As and Sb}$) compounds have, in general, parabolic bands around Fermi level (the parabolic degree is vary from $\text{LaFe}_4\text{P}_{12} \rightarrow \text{LaFe}_4\text{As}_{12} \rightarrow \text{LaFe}_4\text{Sb}_{12}$). The three compounds exhibit a maximum carrier concentration around Fermi level and confirm that the $\text{LaFe}_4\text{X}_{12}$ ($\text{X} = \text{P, As and Sb}$) compounds possess n-/p-types conduction in the energy region $(\mu - E_F)$ confined between ∓ 0.2 eV the region where these compounds expected to give maximum efficiency. It has been noticed that increasing the temperature has insignificant influence on the carriers concentration for $\mu - E_F = \mp 0.2$ eV. In addition, the total density of states in the energy region between 0.2 and -0.2 eV was illustrated in Fig. 1(d) to explore the total density of states around E_F .

The information about the relative position of Fermi level with respect to the principal points of the crystalline Brillouin zone and the dispersion of the bands in the vicinity of E_F are the main criteria for design promising thermoelectric materials. Therefore, in the current work we have investigated the influence of substituting of P by As and As by Sb on the thermoelectric properties of $\text{LaFe}_4\text{X}_{12}$ ($\text{X} = \text{P, As and Sb}$) compounds. We have calculated the effective mass (m^*) and effective mass ratio (m^*/m) for Fe-3d and X-p bands around Γ point the center of the BZ of $\text{LaFe}_4\text{X}_{12}$ ($\text{X} = \text{P, As and Sb}$) compounds. These values are listed in Table 1. It has been found that the effective mass of Fe-3d band for $\text{LaFe}_4\text{Sb}_{12} > \text{LaFe}_4\text{P}_{12} > \text{LaFe}_4\text{As}_{12}$ which implies that the carriers of Fe-3d in $\text{LaFe}_4\text{As}_{12}$ compound possess the highest mobility. Whereas the effective

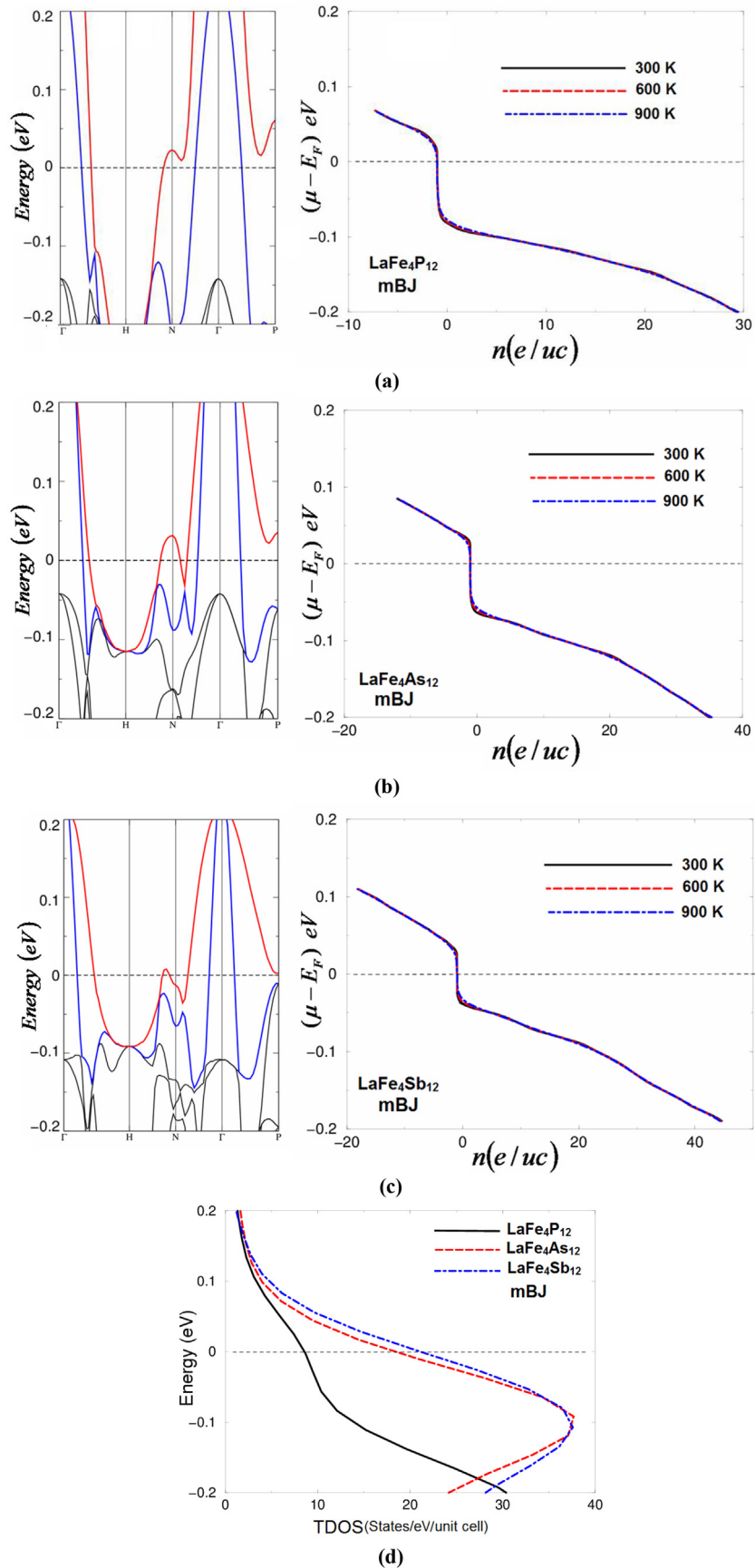


Fig. 1. Calculated electronic band structure of $\text{LaFe}_4\text{X}_{12}$ ($\text{X} = \text{P}, \text{As}$ and Sb) compounds in the vicinity of Fermi level in the energy range between $+0.2$ eV and -0.2 eV; (a) Band structure of $\text{LaFe}_4\text{P}_{12}$ together with the calculated number of carriers concentration at three constant temperatures (300, 600 and 900) K (**we highlight the bands which cuts Fermi**

Table 1

The calculated effective mass $m^* \times 10^{-31}$ and effective mass ratio (m^*/m) around Γ point the center of the BZ for $\text{LaFe}_4\text{X}_{12}$ ($X = \text{P, As and Sb}$) compounds.

$\text{LaFe}_4\text{P}_{12}$		$\text{LaFe}_4\text{As}_{12}$		$\text{LaFe}_4\text{Sb}_{12}$	
m^*/m		m^*/m		m^*/m	
Fe-3d	P-3p	Fe-3d	As-4p	Fe-3d	Sb-5p
0.00480	0.02032	0.00368	0.02097	0.02477	0.00551
$m^* \times 10^{-31}$		$m^* \times 10^{-31}$		$m^* \times 10^{-31}$	
0.04372	0.18498	0.03353	0.19087	0.22547	0.05014

mass for X-p bands is $\text{LaFe}_4\text{As}_{12} > \text{LaFe}_4\text{P}_{12} > \text{LaFe}_4\text{Sb}_{12}$. In other word, for $\text{LaFe}_4\text{P}_{12}$ the carriers of both Fe-3d and P-3p possess intermediate mobility between $\text{LaFe}_4\text{As}_{12}$ and $\text{LaFe}_4\text{Sb}_{12}$ (see Fig. 2(b)). Whereas in $\text{LaFe}_4\text{As}_{12}$ the carriers of Fe-3d possess high mobility and As-4p lowest mobility. For $\text{LaFe}_4\text{Sb}_{12}$ the carriers of Fe-3d possess low mobility and Sb-5p high mobility. That is attributed to the degree of the parabolic of these bands.

3.2. Transport properties

3.2.1. Charge carriers concentration and electrical conductivity

The carriers mobility of $\text{LaFe}_4\text{X}_{12}$ ($X = \text{P, As and Sb}$) compounds were calculated at a certain value of the chemical potential as a function of temperature and carrier concentration as shown in Fig. 2(a) and (b). It has been found that the carriers mobility decreases with increasing the temperature also with increasing the carriers concentration, that is attributed to the fact that at high temperature and high carriers concentration the scattering rate dramatically increases resulting in impediment the carriers mobility. Also we can see that substituting $\text{P} \rightarrow \text{As} \rightarrow \text{Sb}$ lead to reduce the carriers mobility with increasing the temperature (see Fig. 2(a)). While it cause to increase (reduce) the carriers mobility of $\text{LaFe}_4\text{As}_{12}$ ($\text{LaFe}_4\text{Sb}_{12}$) with increasing the carriers concentration (see Fig. 2(b)). The total carriers concentration is defined as the difference between the hole and the electron concentrations. The electron and holes carrier concentration are define as [41]:

$$h = \frac{2}{\Omega} \int_{\text{BZ}} \int_{\text{VB}} [1 - f_0(T, \varepsilon, \mu)] D_v(\varepsilon) d\varepsilon \quad (1)$$

$$e = \frac{2}{\Omega} \int_{\text{BZ}} \int_{\text{CB}} f_0(T, \varepsilon, \mu) D_c(\varepsilon) d\varepsilon \quad (2)$$

In the above equation, the integral is performed over the Brillouin zone (BZ) as well as over conduction band (CB) for electrons (e) or valence band (VB) for holes (h) and Ω is the volume of unit cell. Where $D_v(\varepsilon)$ and $D_c(\varepsilon)$ are the density of states of the valence and the conduction bands. The charge carriers concentration of $\text{LaFe}_4\text{X}_{12}$ ($X = \text{P, As and Sb}$) compounds as a function of temperature at a certain chemical potential is illustrated in Fig. 2(c). It is clear that the charge carrier concentration of $\text{LaFe}_4\text{X}_{12}$ ($X = \text{P, As and Sb}$) compounds increases with increasing the temperature. It has been found that replacing P by As cause significant increases in the carrier concentration with increasing the temperatures, while replacing As by Sb exhibit insignificant increase in the carrier concentration of $\text{LaFe}_4\text{Sb}_{12}$ with respect to $\text{LaFe}_4\text{As}_{12}$. That is

attributed to the fact that the density of states at E_F is the lowest for $\text{LaFe}_4\text{P}_{12}$, also it has high k -dispersion bands for both Fe-3d and P-3p around E_F and thus low effect masses and hence high mobility carriers which could be one reason of reducing the carrier concentration according to the formula $n = \sigma/e\eta$, where n is the carrier concentration, σ the electrical conductivity and η is the mobility. The carrier concentration is indirectly related to the effective masses through the mobility ($\eta_e = e\tau_e/m_e^*$ and $\eta_h = p\tau_h/m_h^*$). The observed carrier concentration of $\text{LaFe}_4\text{X}_{12}$ ($X = \text{P, As and Sb}$) compounds is zero at 50 K, while it is 0.53, 1.37, 1.42 e/uc , respectively at 900 K.

The electrical conductivity ($\sigma = ne\eta$) is directly proportional to the charge carriers density (n) and their mobility (η) therefore, to have the highest electrical conductivity, high $n\eta$ is required. Since $\text{LaFe}_4\text{X}_{12}$ ($X = \text{P, As and Sb}$) compounds have parabolic bands around E_F therefore, we expected to have carriers with low effective mass and high mobility. Also substituting $\text{P} \rightarrow \text{As} \rightarrow \text{Sb}$ lead to increase the density of states around E_F thus we expected to gain high carriers density. Therefore, with substituting $\text{P} \rightarrow \text{As} \rightarrow \text{Sb}$ we expected to achieve high $n\eta$. Fig. 3(a) show that $\text{LaFe}_4\text{P}_{12}$ compound exhibit electrical conductivity reduction with increasing the temperature for a certain value of the chemical potential. Replacing P by As lead to increase electrical conductivity of $\text{LaFe}_4\text{As}_{12}$ with respect to $\text{LaFe}_4\text{P}_{12}$. It is clear that $\text{LaFe}_4\text{As}_{12}$ show the highest electrical conductivity among the other compounds along the temperatures range, that is attributed to the fact that Fe-d band around E_F exhibit high parabolic shape (see Fig. 1(b)) resulting in high mobility in comparison to $\text{LaFe}_4\text{P}_{12}$ and $\text{LaFe}_4\text{Sb}_{12}$. While in $\text{LaFe}_4\text{Sb}_{12}$ compound the Fe-d band show low dispersion (see Fig. 1(c)- low parabolic band) therefore the carriers of this band possess very low mobility resulting in less electrical conductivity as it is clear from Fig. 3(a).

To ascertain the influence of substituting P by As and As by Sb on the electrical conductivity, we have investigated the electrical conductivity as a function of chemical potential at three constant temperatures (300, 600 and 900) K as shown in Fig. 3(b)–(d). It is clear that substituting P by As cause a significant increases in the electrical conductivity in the vicinity of E_F , which confirm our previous observation from Fig. 3(a), due to the high dispersion of Fe-d band in the vicinity of E_F which could be one of the important reasons for increasing the electrical conductivity of $\text{LaFe}_4\text{As}_{12}$ according to the formula $\sigma = ne\eta$. While $\text{LaFe}_4\text{Sb}_{12}$ show the lowest electrical conductivity among the others for the same reason mentioned above (Fig. 3(a)). For all $\text{LaFe}_4\text{X}_{12}$ ($X = \text{P, As and Sb}$) compounds, increasing the temperature has no significant influence on the electrical conductivity in the investigated chemical potential range and the highest value of σ/τ is achieved at 300 K.

3.2.2. Electronic thermal conductivity

To maintain the temperature gradient, a material with low thermal conductivity is required for designing efficient thermoelectric devices. The thermal conductivity is defined as $\kappa = \kappa_e + \kappa_l$, here κ_e is the electronic contribution where both of electrons and holes transporting heat, while κ_l is the lattice contribution (phonons traveling through the lattice). BoltzTraP code calculates only the electronic part κ_e [35]. Fig. 4(a) illustrated the calculated electronic thermal conductivity of $\text{LaFe}_4\text{X}_{12}$ ($X = \text{P, As and Sb}$) compounds as a function of temperature. It has been found that $\text{LaFe}_4\text{As}_{12}$ exhibit higher electronic thermal conductivity among the

level by red and blue colors); (b) Band structure of $\text{LaFe}_4\text{As}_{12}$ together with the calculated number of carriers concentration at three constant temperatures (300, 600 and 900) K (we highlight the bands which cuts Fermi level by red and blue colors); (c) Band structure of $\text{LaFe}_4\text{Sb}_{12}$ together with the calculated number of carriers concentration at three constant temperatures (300, 600 and 900) K (we highlight the bands which cuts Fermi level by red and blue colors); (d) calculated total density of states in the vicinity of Fermi level in the energy range between +0.2 eV and -0.2 eV. (For interpretation of the references to colour in this figure legend, the reader is referred to the web version of this article.)

others along the whole temperatures range at constant chemical potential. While $\text{LaFe}_4\text{Sb}_{12}$ exhibit low electronic thermal conductivity in the temperature range between 50 K up to 600 K, then above 650 K, $\text{LaFe}_4\text{P}_{12}$ compound show the lower electronic thermal conductivity. Overall the electronic thermal conductivity of $\text{LaFe}_4\text{X}_{12}$ ($X = \text{P, As and Sb}$) compounds increases almost linearly with increasing the temperatures. Furthermore, we have investigated the electronic thermal conductivity of $\text{LaFe}_4\text{X}_{12}$ ($X = \text{P, As and Sb}$) compounds as a function of chemical potential in the vicinity of E_F for three constant temperatures as shown in Fig. 4(b)–(d). It has been found that a significant increases in the electronic thermal conductivity of $\text{LaFe}_4\text{X}_{12}$ ($X = \text{P, As and Sb}$) compounds occurs with increasing the temperature from 300 \rightarrow 600 \rightarrow 900 K. The lowest electronic thermal conductivity is achieved at 300 K for the investigated compounds.

3.2.3. Seebeck coefficient (thermopower)

One of the important quantity which is related to the electronic structure of the materials is the Seebeck coefficient (S) or thermopower. In Fig. 5(a) we have illustrated the Seebeck coefficient of $\text{LaFe}_4\text{X}_{12}$ ($X = \text{P, As and Sb}$) compounds as function of temperature at a certain value of chemical potential. It is clear that the Seebeck coefficient of the three compounds increases with increasing the

temperature. Moving from $\text{P} \rightarrow \text{As} \rightarrow \text{Sb}$ cause significant increases in the Seebeck coefficient and $\text{LaFe}_4\text{Sb}_{12}$ compound show the highest Seebeck coefficient along whole temperature scale. At this value of the chemical potential the three compounds represent only p-type conduction.

To investigate the Seebeck coefficient as a function of chemical potential, we have calculated and illustrated the Seebeck coefficient at three constant temperatures (300, 600 and 900) K as shown in Fig. 5(b)–(d). It has been observed that in the investigated interval of the chemical potential where $\mu - E_F = \mp 0.2$ eV, the three compounds represent both of n-type and p-type conduction. The calculated values of Seebeck coefficient in the vicinity of E_F for the n-type and p-type conduction are listed in Table 2. It is clear that $\text{LaFe}_4\text{Sb}_{12}$ present that highest Seebeck coefficient for the n-type and p-type conduction then $\text{LaFe}_4\text{As}_{12}$ comes as the next while the lowest values were for $\text{LaFe}_4\text{P}_{12}$. In all cases the investigated materials exhibit the highest value of Seebeck coefficient at 300 K.

3.2.4. Power factor

The dimensionless figure of merit ($ZT = S^2\sigma T/k$) is very important quantity for calculating the transport properties of the materials [40,41]. The power factor ($P = S^2\sigma/\tau$) comes in the numerator of

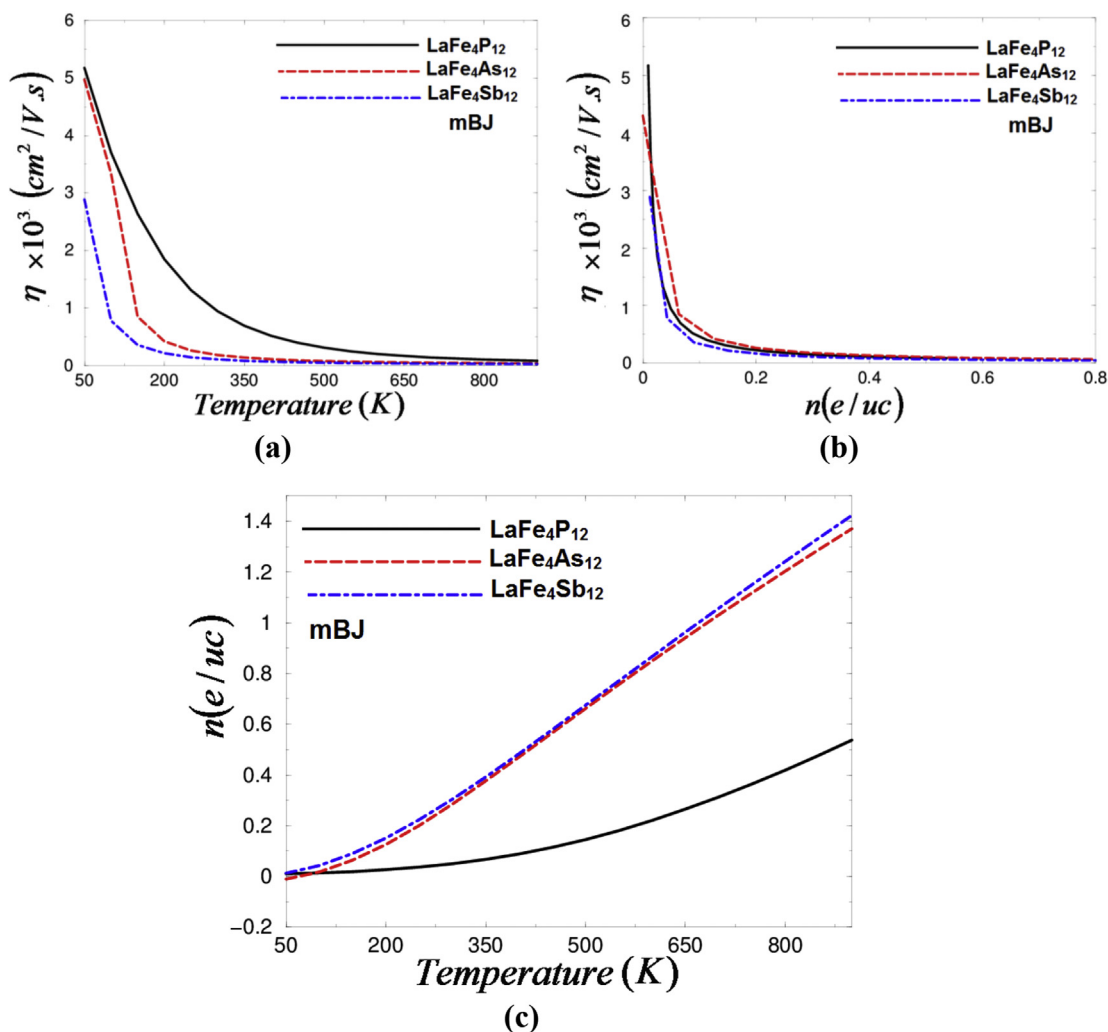


Fig. 2. (a) Calculated mobility as function of temperature at a certain value of chemical potential; (b) Calculated mobility as function of carriers concentration at a certain value of chemical potential; (c) Calculated carriers concentration as function of temperature at a certain value of chemical potential.

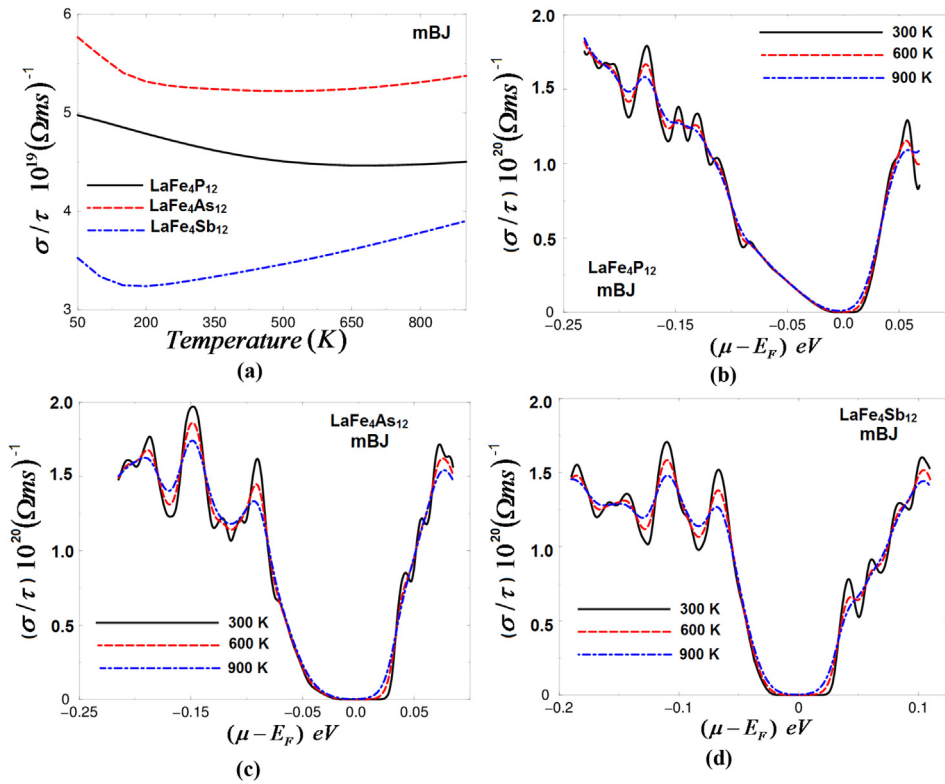


Fig. 3. (a) Calculated electrical conductivity of $\text{LaFe}_4\text{X}_{12}$ ($\text{X} = \text{P}, \text{As}$ and Sb) compounds as a function of temperatures; (b) Calculated electrical conductivity of $\text{LaFe}_4\text{P}_{12}$ as a function of chemical potential at three constant temperatures 300, 600 and 900 K; (c) Calculated electrical conductivity of $\text{LaFe}_4\text{As}_{12}$ as a function of chemical potential at three constant temperatures 300, 600 and 900 K; (d) Calculated electrical conductivity of $\text{LaFe}_4\text{Sb}_{12}$ as a function of chemical potential at three constant temperatures 300, 600 and 900 K.

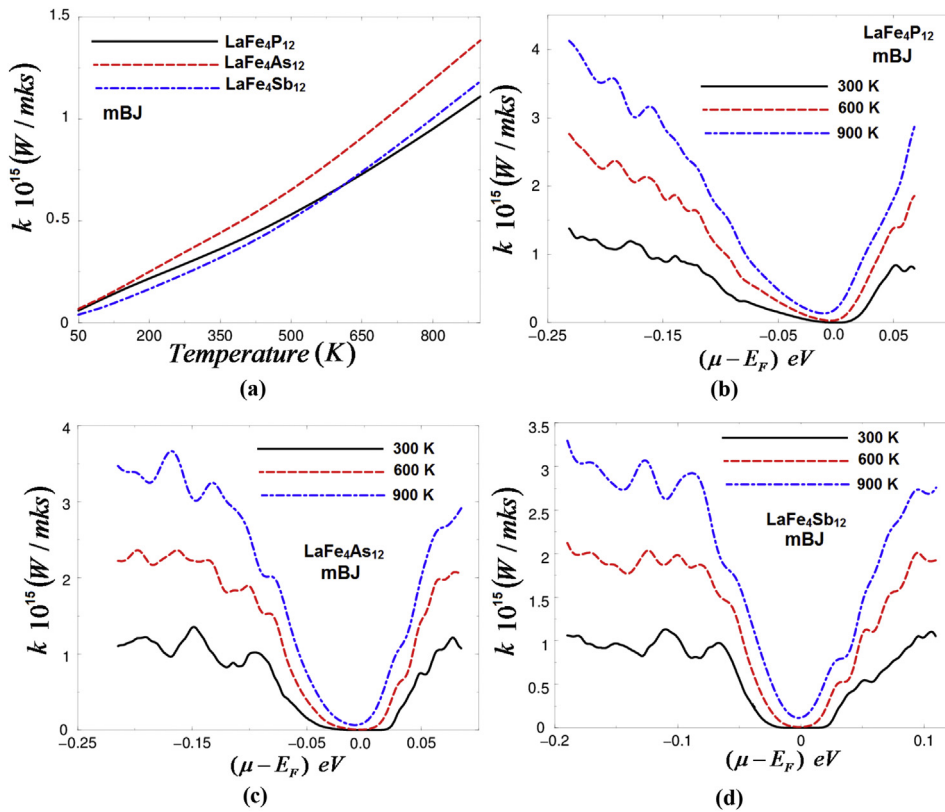


Fig. 4. (a) Calculated electronic thermal conductivity of $\text{LaFe}_4\text{X}_{12}$ ($\text{X} = \text{P}, \text{As}$ and Sb) compounds as a function of temperatures; (b) Calculated electronic thermal conductivity of $\text{LaFe}_4\text{P}_{12}$ as a function of chemical potential at three constant temperatures 300, 600 and 900 K; (c) Calculated electronic thermal conductivity of $\text{LaFe}_4\text{As}_{12}$ as a function of chemical potential at three constant temperatures 300, 600 and 900 K; (d) Calculated electronic thermal conductivity of $\text{LaFe}_4\text{Sb}_{12}$ as a function of chemical potential at three constant temperatures 300, 600 and 900 K.

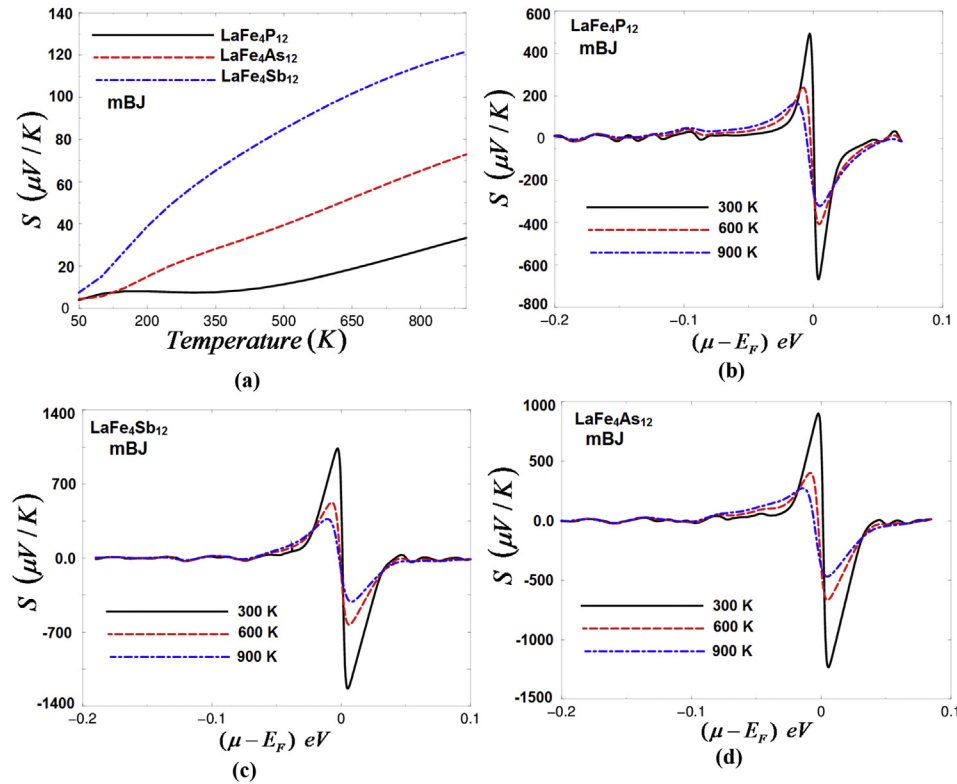


Fig. 5. (a) Calculated Seebeck coefficient of $\text{LaFe}_4\text{X}_{12}$ ($\text{X} = \text{P}, \text{As}$ and Sb) compounds as a function of temperatures; (b) Calculated Seebeck coefficient of $\text{LaFe}_4\text{P}_{12}$ as a function of chemical potential at three constant temperatures 300, 600 and 900 K; (c) Calculated Seebeck coefficient of $\text{LaFe}_4\text{As}_{12}$ as a function of chemical potential at three constant temperatures 300, 600 and 900 K; (d) Calculated Seebeck coefficient of $\text{LaFe}_4\text{Sb}_{12}$ as a function of chemical potential at three constant temperatures 300, 600 and 900 K.

the figure of merit, thus the power factor is an important quantity and play principle role in evaluate the transport properties of the materials. It is clear that the power factor P is directly proportional to S^2 and σ/τ . Therefore, in order to gain high power factor one need to maintain the values of S^2 and σ/τ . Fig. 6 illustrated the calculated power factor of $\text{LaFe}_4\text{X}_{12}$ ($\text{X} = \text{P}, \text{As}$ and Sb) compounds as a function of temperature at certain value of chemical potential. It has been noticed that $\text{LaFe}_4\text{P}_{12}$ exhibit zero power factor up to 450 K while $\text{LaFe}_4\text{As}_{12}$ exhibit zero power factor up to 160 K and $\text{LaFe}_4\text{Sb}_{12}$ up to 75 K. Above these temperature values the power factor of the three compounds increases with increasing the temperature, and $\text{LaFe}_4\text{Sb}_{12}$ compound show the highest power factor along the whole temperature range.

4. Conclusions

The all-electron full-potential linear augmented plane wave plus local orbitals (FP-LAPW + lo) method within the recently modified Becke–Johnson potential (mBJ) were employed to obtain the electronic band structure of $\text{LaFe}_4\text{X}_{12}$ ($\text{X} = \text{P}, \text{As}$ and Sb) compounds. Based on the calculated electronic band structure the electronic transport coefficients were evaluated by utilizing the semi-classical

Boltzmann theory and rigid band model. The carriers concentration (n), Seebeck coefficient (S), electrical conductivity (σ/τ), electronic thermal conductivity (κ_e/τ), and the electronic power factor ($S^2\sigma/\tau$) as a function of temperature at certain value of chemical potential as well as a faction of chemical potential at three constant temperatures (300, 600 and 900) K are theoretically investigated. The information about the relative position of Fermi level with respect to the principal points of the crystalline Brillouin zone and the dispersion of the upper valence bands are the main criteria for design promising thermoelectric materials. Therefore, in the current work we have investigated the influence of substituting of P by

Table 2
Calculated values of Seebeck coefficient $S(\mu\text{V}/\text{K})$ for n-type and p-type conduction of $\text{LaFe}_4\text{X}_{12}$ ($\text{X} = \text{P}, \text{As}$ and Sb) compounds.

$\text{LaFe}_4\text{P}_{12}$		$\text{LaFe}_4\text{As}_{12}$		$\text{LaFe}_4\text{Sb}_{12}$	
n-type	p-type	n-type	p-type	n-type	p-type
674	491	1250	929	1255	1037

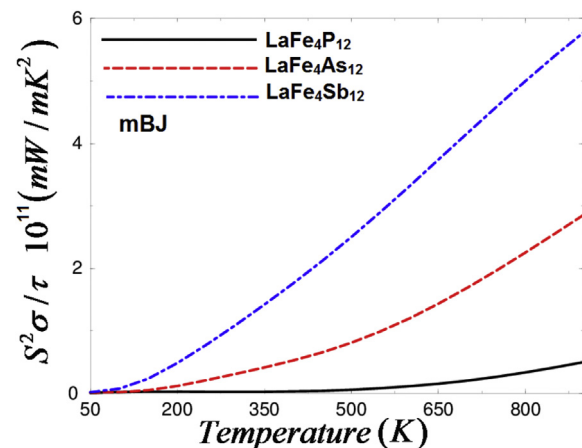


Fig. 6. Calculated power factor of $\text{LaFe}_4\text{X}_{12}$ ($\text{X} = \text{P}, \text{As}$ and Sb) compounds as a function of temperatures.

As and As by Sb on the thermoelectric properties of $\text{LaFe}_4\text{X}_{12}$ ($\text{X} = \text{P}$, As and Sb) compounds. It is interesting to mention that due to the small electro-negativity differences between P, As and Sb therefore, substituting $\text{P} \rightarrow \text{As} \rightarrow \text{Sb}$ will not introduce more peaks in the density of states and no extra charge will be attracted towards As or Sb when we replace P by As and As by Sb. A significant increases in the carriers concentration with increasing temperature occurs when we replace P by As, while substituting As by Sb show insignificant increase in the carriers concentration of $\text{LaFe}_4\text{Sb}_{12}$ with respect to $\text{LaFe}_4\text{As}_{12}$. The highest electrical conductivity was achieved by $\text{LaFe}_4\text{As}_{12}$ compound. It has been noticed that $\text{LaFe}_4\text{Sb}_{12}$ exhibit low electronic thermal conductivity in the temperature range between 50 and 600 K, then above 650 K the $\text{LaFe}_4\text{P}_{12}$ compound show the lower electronic thermal conductivity. The Seebeck coefficient of the three compounds increases with increasing the temperature. Moving from $\text{P} \rightarrow \text{As} \rightarrow \text{Sb}$ cause significant increases in the Seebeck coefficient and $\text{LaFe}_4\text{Sb}_{12}$ compound show the highest Seebeck coefficient and highest power factor along whole temperature scale.

Acknowledgments

The result was developed within the CENTEM project, reg. no. CZ.1.05/2.1.00/03.0088, cofunded by the ERDF as part of the Ministry of Education, Youth and Sports OPRDI programme and, in the follow-up sustainability stage, supported through CENTEM PLUS (LO1402) by financial means from the Ministry of Education, Youth and Sports under the "National Sustainability Programme I. Computational resources were provided by MetaCentrum (LM2010005) and CERIT-SC (CZ.1.05/3.2.00/08.0144) infrastructures.

References

- [1] G.D. Mahan, H. Ehrenreich, F. Spaepen (Eds.), *Solid State Physics* vol. 51, Academic Press, New York, 1998, p. 81.
- [2] B.C. Sales, D. Mandrus, B.C. Chakoumakos, V. Keppens, J.R. Thompson, *Phys. Rev. B* 56 (1997) 15081.
- [3] G.S. Nolas, J.L. Cohn, G.A. Slack, *Phys. Rev. B* 58 (1998) 164.
- [4] G.P. Meisner, M.S. Torikachvili, K.N. Yang, M.B. Maple, R.P. Guertin, *J. Appl. Phys.* 57 (1985) 3073.
- [5] I. Shirotni, T. Uchiumi, C. Sekine, S. Kimura, N. Hamaya, *J. Solid State Chem.* 142 (1999) 146.
- [6] I. Shirotni, T. Uchiumi, K. Ohno, C. Sekine, Y. Nakazawa, K. Kanoda, S. Todo, T. Yagi, *Phys. Rev. B* 56 (1997) 7866.
- [7] T. Uchiumi, I. Shirotni, C. Sekine, S. Todo, T. Yagi, Y. Nakazawa, K. Kanoda, *J. Phys. Chem. Solids* 60 (1999) 689.
- [8] E.D. Bauer, N.A. Frederick, P.-C. Ho, V.S. Zapf, M.B. Maple, *Phys. Rev. B* 65 (2002) 100506R.
- [9] M.S. Torikachvili, C. Rossel, M.W. McElfresh, M.B. Maple, R.P. Guertin, G.P. Meisner, *J. Magn. Magn. Mater* 54 (1986) 365.
- [10] M.E. Danebrock, C.B.H. Evers, W. Jeitschko, *J. Phys. Chem. Solids* 57 (1996) 381.
- [11] L. Keller, P. Fischer, T. Herrmannsdörfer, A. Dönni, H. Sugawara, T.D. Matsuda, K. Abe, Y. Aoki, H. Sato, *J. Alloys Compd.* 323 (2001) 516.
- [12] K. Tenya, N. Oeschler, P. Gegenwart, F. Steglich, N.A. Frederick, E.D. Bauer, M.B. Maple, *Acta Phys. Pol. B* 34 (2003) 995.
- [13] C. Sekine, T. Uchiumi, I. Shirotni, K. Matsuhira, T. Sakakibara, T. Goto, T. Yagi, *Phys. Rev. B* 62 (2000) 11581.
- [14] C. Sekine, T. Uchiumi, I. Shirotni, T. Yagi, *Phys. Rev. Lett.* 79 (1997) 3218.
- [15] S.V. Dordevic, D.N. Basov, N.R. Dilley, E.D. Bauer, M.B. Maple, *Phys. Rev. Lett.* 86 (2001) 684.
- [16] A. Yamasaki, S. Imada, T. Masuda, T. Nanba, A. Sekiyama, H. Sugawara, T.D. Matsuda, H. Sato, C. Sekine, I. Shirotni, H. Harima, S. Suga, *Acta Phys. Pol. B* 34 (2003) 1035.
- [17] E.D. Bauer, A. Slebarski, E.J. Freeman, C. Sirvent, M.B. Maple, *J. Phys. Condens. Matter* 13 (2001) 4495.
- [18] F. Grandjean, A. Gérard, D.J. Braun, W. Jeitschko, *J. Phys. Chem. Solids* 45 (1984) 877.
- [19] W. Jeitschko, D.J. Braun, *Acta Crystallogr.* 33 (1977) 3401.
- [20] B.C. Sales, D. Mandrus, B.C. Chakoumakos, V. Keppens, J.R. Thompson, *Phys. Rev. B* 56 (1997) 15081.
- [21] G.S. Nolas, J.L. Cohn, G.A. Slack, *Phys. Rev. B* 58 (1998) 164.
- [22] K. Nouneh, Ali H. Reshak, S. Auluck, I.V. Kityk, R. Vienneis, S. Benet, S. Charar, *J. Alloys Compd.* 437 (2007) 39–46.
- [23] T. Caillat, A. Borshchevsky, J.P. Fleurial, in: *Proceedings of the 11th International Conference on Thermoelectrics*, Arlington, USA, 7–9 October, 1992, p. 3. G.J. Snyder, T. Caillat, *Using The Compatibility Factor To Design High Efficiency Segmented Thermoelectric Generators Materials Research Society Symposium Proceedings*, vol. 793, 2003, p. 37.
- [24] K. Nouneh, R. Vienneis, I.V. Kityk, F. Terki, S. Charar, S. Benet, S. Paschen, *Phys. Stat. Sol.(b)* 241 (13) (2004) 3069–3080.
- [25] Hisatomo Harima, Katsuhiko Takegahara, *Phys. B* 328 (2003) 26–28.
- [26] Katsuhiko Takegahara, Hisatomo Harima, *J. Magnetism Magnetic Mater.* 310 (2007) 861–863.
- [27] M. Hachemaoui, R. Khenata, A. Bouhemadou, S. Bin-Omran, Ali H. Reshak, F. Semari, D. Rached, *Solid State Commun.* 150 (2010) 1869–1873.
- [28] A.H. Reshak, M. Piasecki, S. Auluck, I.V. Kityk, R. Khenata, B. Andriyevsky, C. Cobet, N. Esser, A. Majchrowski, O.M.S. Wirkowicz, R. Diduszko, W. Szyrski, *J. Phys. Chem. B* 113 (2009) 15237–15242.
- [29] F. Tran, P. Blaha, *Phys. Rev. Lett.* 102 (2009), 226401.
- [30] A.H. Reshak, A. Majchrowski, M. Swirkowicz, A. Ktos, T. Łukasiewicz, I.V. Kityk, K. Iliopoulos, S. Courise, M.G. Brik, *J. Alloys Compd.* 481 (2009) 14–16.
- [31] A.H. Reshak, S. Auluck, I.V. Kityk, *J. Alloys Compd.* 473 (2009) 20–24.
- [32] Y. Saeed, S. Nazir, A.H. Reshak, A. Shaikat, *J. Alloys Compd.* 508 (2010) 245–250.
- [33] A.H. Reshak, H. Kamarudin, S. Auluck, *J. Alloys Compd.* 509 (2011) 9685–9691.
- [34] A.H. Reshak, *RSC Adv.* 5 (2015) 33632.
- [35] G.K.H. Madsen, D.J. Singh, *Comput. Phys. Commun.* 175 (2006) 67–71.
- [36] B. Xu, X. Li, G. Yu, J. Zhang, S. Ma, Y. Wang, L. Yi, *J. Alloys Compd.* 565 (2013) 22–28.
- [37] A.H. Reshak, *Opt. Mater.* 47 (2015) 453–461.
- [38] P. Blaha, K. Schwarz, G.K.H. Madsen, D. Kvasnicka, J. Luitz, WIEN2k, an Augmented Plane Wave Plus Local Orbitals Program for Calculating Crystal Properties, Vienna University of Technology, Austria, 2001.
- [39] J.P. Perdew, A. Zunger, *Phys. Rev. B* 23 (1981) 5048.
- [40] Joo-Hyoung Lee, Junqiao Wu, Jeffrey C. Grossman, *PRL* 104 (016602) (2010).
- [41] Chenming Calvin Hu, *Modern Semiconductor Devices for Integrated Circuits, Part I: Electrons and Holes in a Semiconductor*, November 11, 2011.